Nanochem Res 7(1): 36-43, Winter and Spring 2022

RESEARCH PAPER

Triclosan Adsorption on C60 Nanocage: NBO, Thermodynamic, Structural and Electronic Properties

Razieh Razavi

Department of Chemistry, Faculty of Science, University of Jiroft, Jiroft, Iran

ARTICLE INFO

Article History:
Received 26 January 2022
Accepted 22 March 2022
Published 1 May 2022

Keywords:
DFT
Triclosan
C60
Bucky ball
Reactivity
Stability

ABSTRACT

In this study, DFT, B3LYP/6-311++G(2d,2p) was used for discovering the reactivity properties and doping of triclosan on C60 (ih) in gas and water phases. Chemical structure (dipole momentum), thermodynamic properties (Gibbs free energy, enthalpy, entropy and thermal capacity), electronic parameters (σ, μ, ω, χ, and η), NBO, and IR spectrum were calculated. According to the calculated HOMO and LUMO energies, triclosan is stable and reactive. Triclosan has seven active sites all of which are thermodynamically stable.

How to cite this article
Razavi R. Triclosan Adsorption on C60 Nanocage: NBO, Thermodynamic, Structural and Electronic Properties. Nanochem Res, 2022; 7(1):36-43. DOI: 10.22036/ncr.2022.01.006

INTRODUCTION

Triclosan (TCS)[1–3], which is antimicrobial [4] and has low toxicity [5], is used as an additive in care products and medical disinfectants [6-7]. Strong degradation of TCS in short term has resulted in increasing amounts of it in nature [8] [9]. Triclosan (TCS) is used widely in antimicrobial and fungicidal ingredient such as soaps , detergents [10], toothpastes, and cosmetics [11]. Many methods have recently been proposed to remove TCS effectively including biodegradation [12-13], photolysis [14], adsorption [15], and advanced oxidation [16-17]. Triclosan, which is a special and popular antifungal agent and antibacterial [18][19], has drawn public attention due to its wide usage in personal care products and possible removal and disposal in water [20-22]. High technologies such as biological oxidation [23-24], treatment [25], and adsorption [26] by activated carbon (AC)[27-28] and carbon nanotubes [29, 12] have been applied to treat water [30] containing triclosan. However, the adsorption of triclosan by high-silica zeolites has not yet been reported in the literature.

Bucky ball (C60) was applied as absorbant [31-32] for some toxic and nontoxic chemical ingredient [33] in dies [34] and wastewater [7, 22] [35][36]. Density functional theory [37-41] and molecular dynamic calculation [42, 9, 43-44] were used for theoretical calculation in all fields of study [45] such as nanocage[31].

In this study, bucky ball(C60) was used as an absorbant of triclosan in gas and water phases by density functional theory with 6-311++G(2d,2p) basis set.

Computational method

The chemical quantum calculations were applied due to the Gaussian 03 (46) package which was run on a supercomputer. The full geometry

* Corresponding Author Email: *r.razavi@ujiroft.ac.ir*

optimization, electric field gradient, NBO analysis, thermodynamic properties, electronical parameters, and IR spectrum were carried out by the density functional theory (DFT) with three parameter hybrid functionals of Becke B3LYP and the 6-311++g(2d,2p) basis set. Bucky ball C-C (C60 ih) was applied as an absorbant in this study. Adsorption energy was calculated by the following formula:

$$E_{ads}=E_{(B-T)}-(E_{triclosan}+E_{backyball})$$

RESULTS AND DISCUSSION

In previous studies, results of calculations have shown that the adoption of nanocages with metallic atoms can efficiently modify their electrical properties, chemical activity, and reaction potential [47]. Therefore, in this study, all structures such as triclosan, bucky ball (C60, fullerene), and adopted triclosan on bucky ball were optimized by B3LYP/6-311++G(2d,2p). Fig. 1 shows the optimized structure of triclosan in which there are seven active sites in triclosan including three Cl atoms, an OH and an O functions, and two phenyl rings. These seven places have different chemical and electrochemical positions in triclosan. Fig. 2 illustrates all active positions in triclosan. The density of electron in each position has different effects on the chemical reaction. The presence of two phenyl rings with different functional groups can lead to better chemical reactivity in gas phase and solvent phases. HOMO and LUMO density

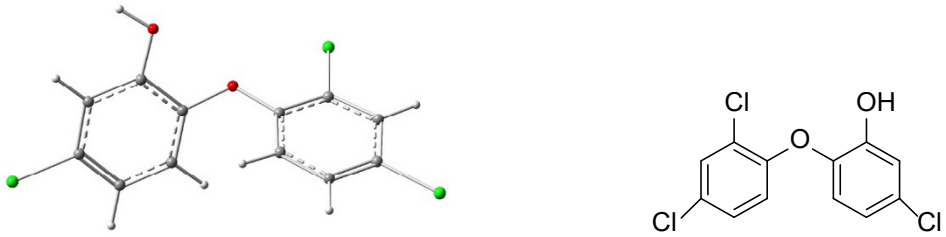

Fig. 1. Optimized structure of triclosan by B3LYP/6-311++G(2d,2p)

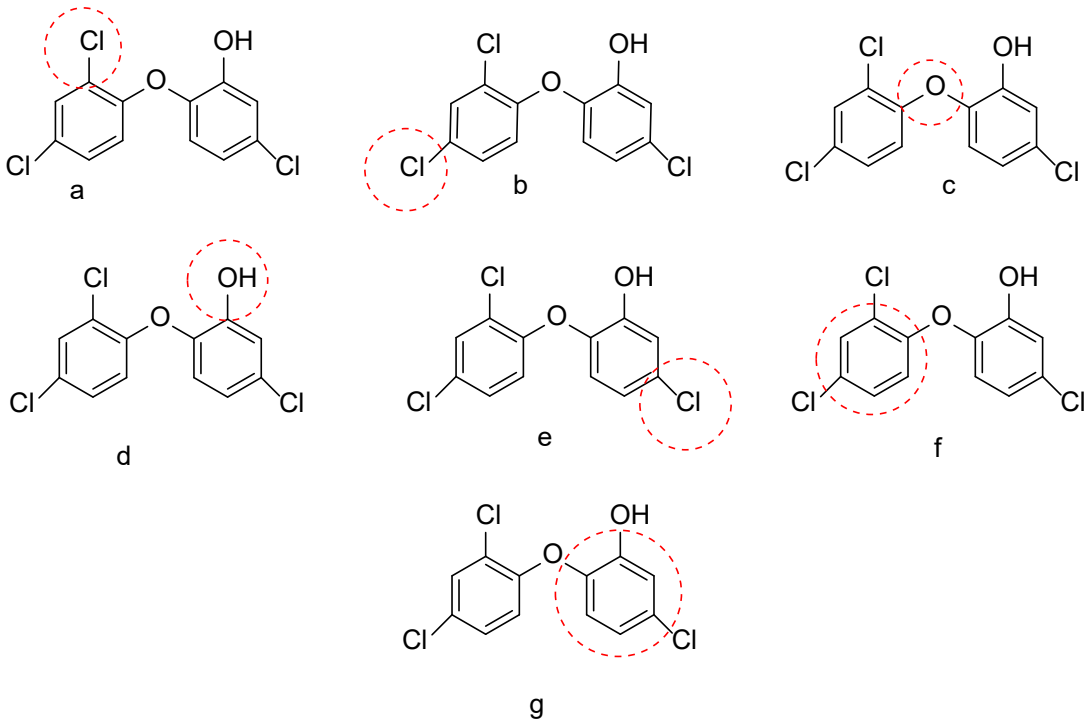

Fig. 2. Different active places in triclosan

electron is demonstrated in Fig. 3 and showed positive and negative position in triclosan. The red color shows negative side and green color shows positive side for reaction. Negative side is electron donating place and positive side is electron philicity place in triclosan. Based on Fig. 3, phenyl ring, which has OH and Cl functions, acts as a donating place in triclosan and phenyl ring which has two chlorine atoms react as positive position in triclosan. The HOMO energy, which is -7.89 and -4.37 eV in water and gas phases, respectively, demonstrates the strong reactivity of triclosan.

Important characters in chemical reactivity are HOMO and LUMO energies. The large amount of LUMO shows that a molecule is more electron accepting. HOMO and LUMO energies can recognize and predict the strength and stability of chemical compounds. According to the energies of these frontier orbitals, which are the nearby orbitals with various levels of energy, the HOMO-LUMO band gap energy is where the most electron excitations can occur. In particular, when there is a large chemical and aromatic system, small HOMO-LUMO band gaps enable the π electrons to jump to the next higher level of energy. The higher mobility of π electrons in large conjugated π orbital systems leads to the greater distribution of the energy throughout the molecule which increases stability. Hence, smaller HOMO-LUMO gaps correspond to better stability. In addition, this mobility of the π electrons means that large aromatic systems (like graphene nanoribbons) have good conductivity and can make great semiconductors since their conduction band gap is small, HOMO and LUMO are fascinating aspects of chemistry which can provide a remarkable insight into the working of reactions based on how orbitals interact to control the outcome of reactions. HOMO energy provides weak electron to react in chemical reactions. Due to its amount of HOMO energy, triclosan participate strongly in chemical reactions; it also has an electron donating role in all chemical reactions due to its electronegative atoms (O, Cl). Table 1 shows the data regarding the triclosan frontier (HOMO and LUMO) orbitals.

A natural bond orbital or NBO is a calculated bonding orbital with maximum electron density. Red placed atoms refer to the negative side and green placed atoms denote the positive side in the structure of triclosan (Fig. 4). According to NBO electron contribution all three Cl are active sides for electron donating and makes the close neighborhood a negative side for chemical reactions.

Fig. 5 compares the predicted IR spectrum with the real one. O-H function appears strongly in 3000 to 3500 cm^{-1}, and C-H aromatic appears weakly in 1650- 2000 cm^{-1}.

Chemical parameters (Table 1) and thermodynamic properties (Table 2) can help chemists to decide about the reactivity of chemical compounds. The dipole momentum of chemical compounds introduce polarity of compounds in reaction media. Based on the data in Table 1,

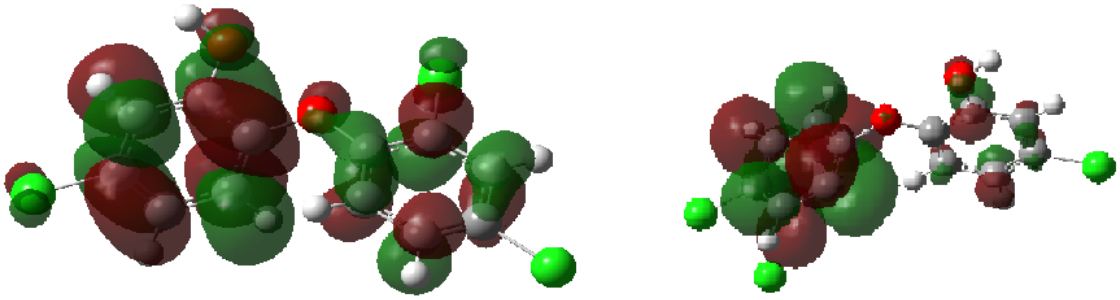

Fig. 3. HOMO and LUMO patterns in gas and water phases by B3LYP/6-311++G(2d,2p)

Table 1. Energy data and dipole momentum of triclosan by B3LYP/6-311++G(2d,2p)

Triclosan	(solvent) water	gas
Energy	-5233.50kJ	-5232.55kJ
Dipole moment	38.1054D	7.7221D
HOMO	-7.89eV (-0.28990) a.u	-4.52eV (-0.16596) a.u
LUMO	-4.37eV (-0.16049) a.u	-4.12eV (-0.15146) a.u

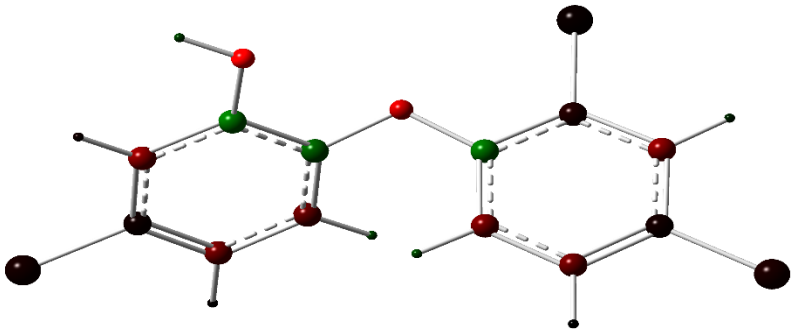

Fig 4. NBO contribution of triclosan electron by B3LYP/6-311++G(2d,2p)

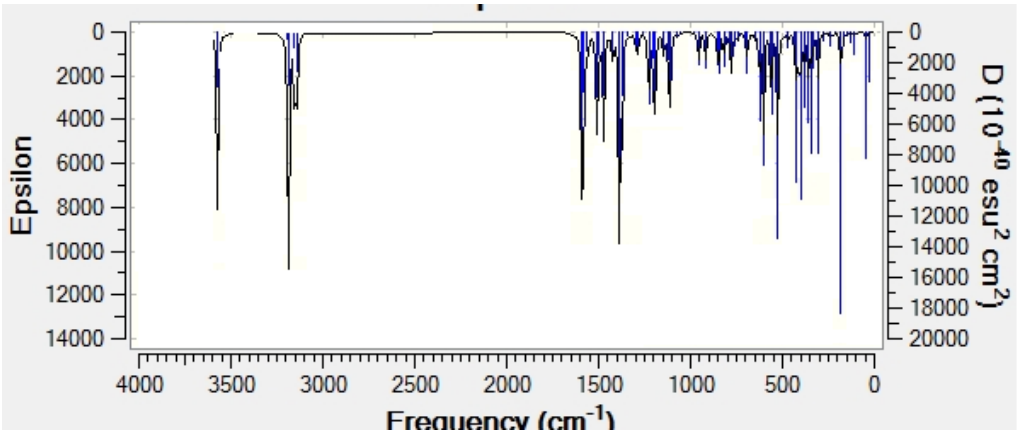

Fig. 5. IR spectrum of triclosan by B3LYP/6-311++G(2d,2p)

Table 2. Thermodynamic parameters of triclosan by B3LYP/6-311++G(2d,2p)

	ΔG	ΔH	ΔS	Cv	lnQ
Triclosan	-5232.26kJ	-5232.09kJ	127.718cal/mol.K	57.514cal/mol.K	-118.758

the dipole momentum of triclosan is 38.105 D in water solution which is higher than the dipole momentum in gas phase (7.722 D). It shows the polarity of triclosan because of the electronegative atoms in its chemical structure (Cl atom). The -OH functional group can make hydrogen bonding with water molecules. Hydrogen bonding and high dipole momentum lead to higher strength and reactivity. Table 2 demonstrates thermodynamic parameters which shows the stability of triclosan.

Fig. 6 illustrates that triclosan has seven active positions for adopting C60 which is (ih) a symmetric system, and all places has the same situation to participate in chemical reactions. Fig. 7 shows the main and optimized structure of bucky ball.

Energy is the capacity of doing work and supplementing heat. Chemical potential energy is saved energy in chemical bonds. Chemical potential is a an important thermodynamic property and an applicable concept to many materials sciences such as chemistry, physics, biology and chemical engineering. All of the thermodynamic parameters of a chemical material at a specific pressure and temperature can be calculated from chemical potential. Under the condition of constant pressure and temperature, chemical potential determines the stability of substances, chemical compounds, and solutions. The value of chemical potential (μ) for triclosan is -260.11 and -396.08 eV in gas and water phases, respectively, and triclosan is a stable chemical compound in both phases. Negative energy

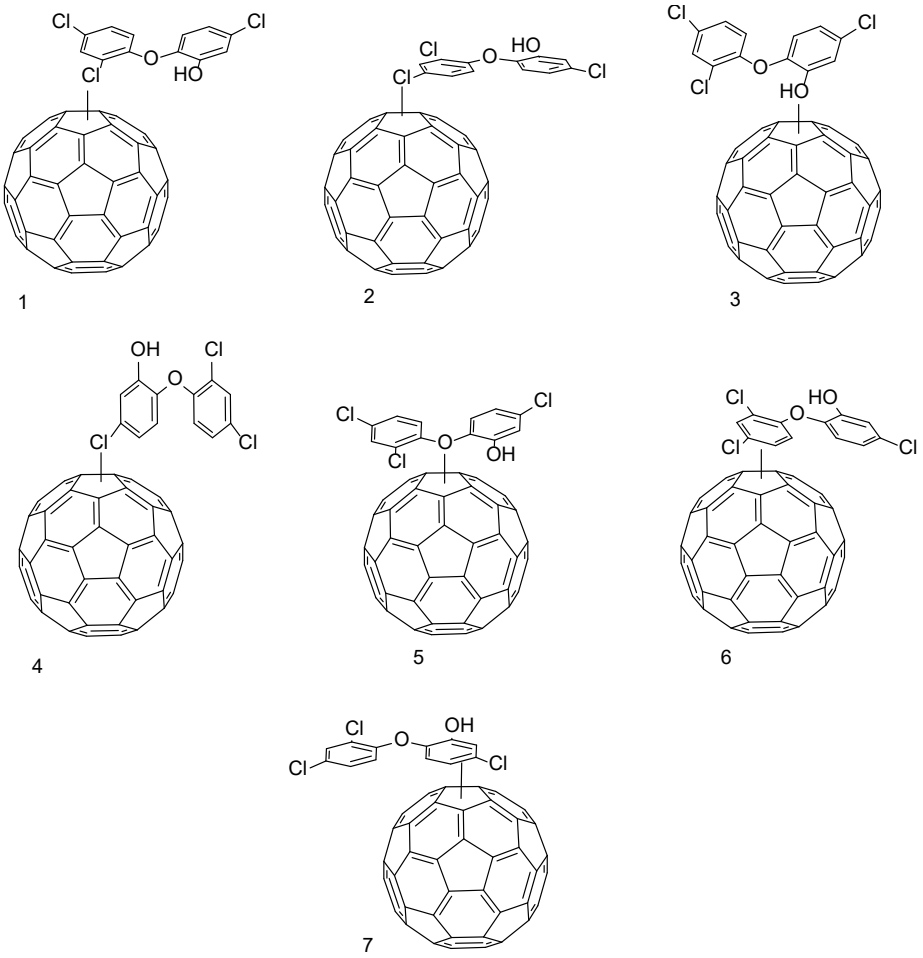

Fig. 6. Triclosan-C60 complexes in different active sides (seven different position)

Table 3. Electronic parameters of triclosan in gas and water phase by B3LYP/6-311++G(2d,2p)

Triclosan	IP (eV)	EA (eV)	μ (eV)	η (eV)	χ (eV)	σ (eV)	ω (eV)
gas	4.52	4.12	-4.32	0.2	4.32	5.00	46.65
water	7.89	4.37	-6.13	1.76	6.13	0.57	10.67

Table 4. Energy of Triclosan-C60 complexes in different active sides

	1	2	3	4	5	6	7
E(kcal/mol)	-1004.214	-1001.206	-1004.380	-806.693	-1165.033	-1000.439	-586.774
μ(D)	1.7817	1.8481	1.6730	1.9957	0.5943	1.8119	1.6412
ΔE(ads/kJ)	-10172.51	-10159.93	-10173.21	-9376.09	-10845.38	-10156.71	-8425.94

shows the hidden energy in the chemical bonds of triclosan. The energy of an atom is determined when it loses or gains energy through chemical reactions that results in losing or gaining electrons. A chemical reaction that releases energy is called an exothermic reaction and a chemical reaction that absorbs energy is called an endothermic reaction. Energy from an exothermic reaction is negative, thus energy is given a negative sign; whereas energy from an endothermic reaction is positive, and energy is given a positive sign. When an electron is added to a neutral atom (i.e., first electron affinity)

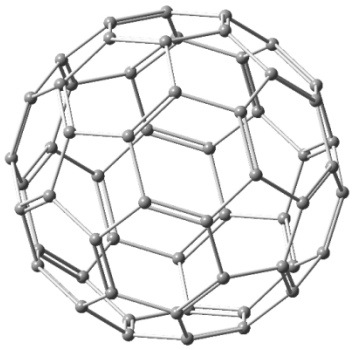

Fig. 7. Optimized structure of C60(ih) by B3LYP/6-311++G(2d,2p) E(-738.33kJ)

energy is released; thus, the first electron affinities are negative. However, more energy is required to add an electron to a negative ion (i.e., second electron affinity) which overwhelms the release of energy from the electron attachment process; therefore, second electron affinities are positive. Triclosan has positive electron affinity energy (EA) which means that it does not want to give electron, rather it wants to donate it. Reactivity parameters of a molecule such as electronegativity (χ), softness (σ), hardness (η), and electrophilicity index (ω) have been extracted from the theory of Koopman by the DFT popular method. Electronegativity (χ) is the value of attraction power of an atom or molecule achieved from HOMO and LUMO. η is responsible for the stability and reactivity of a chemical molecule. σ illustrates the capacity of chemical molecules for accepting electrons. Table 3 shows reactivity parameters of triclosan in gas and water phases. According to these results, it was found that triclosan has high stability and reactivity in chemical reactions. Triclosan was adopted on C60. Table 4 demonstrates the energy of each complex in Fig. 6. In addition, the dipole momentum of each complex indicates that all active sides can act in polar media as well. The relative adopting energy shows that all active sides are stable structures in the chemical media, and structure 5 is the most stable one. The energy of an electron in a single atom can be determined solely by the principal quantum number. However, the energy of an electron in multi-electron atoms depends on both its principal quantum number (n) and its azimuthal quantum number. This difference in energy of various subshells residing in the same shell is mainly attributed to the mutual repulsion among the electrons in a multi-electron atom. In multi-electron atoms, there is a repulsive force acting between various electrons apart from the attractive force between the nucleus and the electrons. Thus, the stability of an electron in a multi-electron atom depends on the total attractive and repulsive interactions. The electron in an atom is only stable when the total attractive interaction is more than the total repulsive interaction. For bigger atoms, due to the presence of electrons in the inner shells, the electrons in the outer shell are deprived of experiencing the full positive charge of the nucleus. This effect is known as the shielding of the outer shell electrons from the nucleus by the inner shell electrons. The net positive charge experienced by the outer shell electrons is termed the effective nuclear charge.

CONCLUSION

The present work considered the chemical reactivity of triclosan and adopting it on bucky ball (C60) which was applied by DFT B3LYP/6-311++G(2d,2p) in gas and water phases. The results of chemical structure, thermodynamic properties, electronic parameters, and IR spectrum demonstrated that triclosan is an active molecule which can be adsorbed on C60 as a stable compound. Triclosan has seven active sides all of which are thermodynamically stable, and structure 5 is the most stable one among other structures.

REFERENCES

[1] Latosińska JN, Tomczak MA, Kasprzak J. Thermal stability and molecular dynamics of triclosan in solid state studied by 35Cl–NQR spectroscopy and DFT calculations. Chemical Physics Letters. 2008;462(4):284-8.

[2] Tabari SA, Esfahani ML, Hosseini SM, Rahimi A. Neurobehavioral toxicity of triclosan in mice. Food and Chemical Toxicology. 2019;130:154-60.

[3] Rodriguez F, Saffon N, Sammartino JC, Degiacomi G, Pasca MR, Lherbet C. First triclosan-based macrocyclic inhibitors of InhA enzyme. Bioorganic Chemistry. 2020;95:103498.

[4] Guo X, Cheng Q, Yu G, Wang H, Tian Z, Shi Z, et al. The functions of hydrophobic elastic polyurethane combined with an antibacterial triclosan derivative in the dentin restoration interface. Journal of the Mechanical Behavior of Biomedical Materials. 2020;102:103471.

[5] Zhang M, Zhu R, Zhang L. Triclosan stimulates human vascular endothelial cell injury via repression of the PI3K/Akt/mTOR axis. Chemosphere. 2020;241:125077.

[6] Fan C, Zhou M, Tang X, Zeng G, Xu Q, Song B, et al. Triclosan enhances short-chain fatty acid production from sludge fermentation by elevating transcriptional activity of acidogenesis bacteria. Chemical Engineering Journal. 2020;384:123285.

[7] Wang S, Poon K, Cai Z. Removal and metabolism of triclosan by three different microalgal species in

aquatic environment. Journal of Hazardous Materials. 2018;342:643-50.
[8] Xin X, Huang G, An C, Raina-Fulton R, Weger H. Insights into long-term toxicity of triclosan to freshwater green algae in Lake Erie. Environmental science & technology. 2019;53(4):2189-98.
[9] Wang C, Huang W, Lin J, Fang F, Wang X, Wang H. Triclosan-induced liver and brain injury in zebrafish (Danio rerio) via abnormal expression of miR-125 regulated by PKCα/Nrf2/p53 signaling pathways. Chemosphere. 2020;241:125086.
[10] Zhang X NLc, Li B, Liu L, Cheng X. Design and construction of a highly efficient photoelectrocatalytic system based on dual-Pd/TNAs photoelectrodes for elimination of triclosan. Separation and Purification Technology. 2020;235:116232.
[11] Zhou X, Xu D, Chen Y, Hu Y. Enhanced degradation of triclosan in heterogeneous E-Fenton process with MOF-derived hierarchical Mn/Fe@PC modified cathode. Chemical Engineering Journal. 2020;384:123324.
[12] Zhao H, Wang L, Kong D, Ji Y, Lu J, Yin X, et al. Degradation of triclosan in a peroxymonosulfate/Br− system: Identification of reactive species and formation of halogenated byproducts. Chemical Engineering Journal. 2020;384:123297.
[13] Wang L, Liu Y, Wang C, Zhao X, Mahadeva GD, Wu Y, et al. Anoxic biodegradation of triclosan and the removal of its antimicrobial effect in microbial fuel cells. Journal of Hazardous Materials. 2018;344:669-78.
[14] Constantin LA, Nitoi I, Cristea NI, Constantin MA. Possible degradation pathways of triclosan from aqueous systems via TiO2 assisted photocatalyis. Journal of Industrial and Engineering Chemistry. 2018;58:155-62.
[15] Dou R, Zhang J, Chen Y, Feng S. High efficiency removal of triclosan by structure-directing agent modified mesoporous MIL-53(Al). Environmental Science and Pollution Research. 2017;24(9):8778-89.
[16] Wang S, Wang J. Activation of peroxymonosulfate by sludge-derived biochar for the degradation of triclosan in water and wastewater. Chemical Engineering Journal. 2019;356:350-8.
[17] Peng J, Zhang Y, Zhang C, Miao D, Li J, Liu H, et al. Removal of triclosan in a Fenton-like system mediated by graphene oxide: Reaction kinetics and ecotoxicity evaluation. Science of The Total Environment. 2019;673:726-33.
[18] Zhu L SY, Xiao H, Santiago-Schübel B, Meyer-Alert H, Schiwy S, et al. Electrochemical simulation of triclosan metabolism and toxicological evaluation. Sci Total Environ 2018;622–623:1193–201.
[19] McCagherty J, Yool DA, Paterson GK, Mitchell SR, Woods S, Marques AI, et al. Investigation of the in vitro antimicrobial activity of triclosan-coated suture material on bacteria commonly isolated from wounds in dogs. American Journal of Veterinary Research. 2020;81(1):84-90.
[20] San-Román MF, Solá-Gutiérrez C, Schröder S, Laso J, Margallo M, Vázquez-Rowe I, et al. Potential formation of PCDD/Fs in triclosan wastewater treatment: An overall toxicity assessment under a life cycle approach. Science of The Total Environment. 2020;707:135981.
[21] Jiang N, Shang R, Heijman SGJ, Rietveld LC. Adsorption of triclosan, trichlorophenol and phenol by high-silica zeolites: Adsorption efficiencies and mechanisms. Separation and Purification Technology. 2020;235:116152.
[22] Adolfsson-Erici M, Pettersson M, Parkkonen J, Sturve J. Triclosan, a commonly used bactericide found in human milk and in the aquatic environment in Sweden. Chemosphere. 2002;46(9):1485-9.
[23] Suarez S, Dodd MC, Omil F, von Gunten U. Kinetics of triclosan oxidation by aqueous ozone and consequent loss of antibacterial activity: Relevance to municipal wastewater ozonation. Water Research. 2007;41(12):2481-90.
[24] Wu Q, Shi H, Adams CD, Timmons T, Ma Y. Oxidative removal of selected endocrine-disruptors and pharmaceuticals in drinking water treatment systems, and identification of degradation products of triclosan. Science of The Total Environment. 2012;439:18-25.
[25] Ying G-G, Kookana RS. Triclosan in wastewaters and biosolids from Australian wastewater treatment plants. Environment International. 2007;33(2):199-205.
[26] Li Y, Liu S, Wang C, Ying Z, Huo M, Yang W. Effective column adsorption of triclosan from pure water and wastewater treatment plant effluent by using magnetic porous reduced graphene oxide. Journal of Hazardous Materials. 2020;386:121942.
[27] Behera SK, Oh S-Y, Park H-S. Sorption of triclosan onto activated carbon, kaolinite and montmorillonite: Effects of pH, ionic strength, and humic acid. Journal of Hazardous Materials. 2010;179(1):684-91.
[28] Liu Y, Zhu X, Qian F, Zhang S, Chen J. Magnetic activated carbon prepared from rice straw-derived hydrochar for triclosan removal. RSC Advances. 2014;4(109):63620-6.
[29] Cho H-H, Huang H, Schwab K. Effects of Solution Chemistry on the Adsorption of Ibuprofen and Triclosan onto Carbon Nanotubes. Langmuir. 2011;27(21):12960-7.
[30] Zheng G, Yu B, Wang Y, Ma C, Chen T. Removal of triclosan during wastewater treatment process and sewage sludge composting—A case study in the middle reaches of the Yellow River. Environment International. 2020;134:105300.
[31] Kang S-H, Kim G, Kwon Y-K. Adsorption properties of chalcogen atoms on a golden buckyball Au_{16}(-) from first principles. J Phys Condens Matter. 2011;23(50):505301.
[32] Gökpek Y, Bilge M, Bilge D, Alver Ö, Parlak C. Adsorption mechanism, structural and electronic properties: 4-Phenylpyridine & undoped or doped (B or Si) C60. Journal of Molecular Liquids. 2017;238:225-8.
[33] Mallawaarachchi S, Premaratne M, Maini PK. Superradiant Cancer Hyperthermia Using a Buckyball Assembly of Quantum Dot Emitters. IEEE Journal of Selected Topics in Quantum Electronics. 2019;25(2):1-8.
[34] Ebrahimi F. Nanocomposites : New Trends and Developments: In Tech; 2012.
[35] Zhao M, Huang Z, Wang S, Zhang L, Wang C. Experimental and DFT study on the selective adsorption mechanism of Au(III) using amidinothiourea-functionalized UiO-66-NH_2. Microporous and Mesoporous Materials. 2020;294:109905.
[36] Khataee HR, Ibrahim MY, Sourchi S, Eskandari L, Teh Noranis MA. Computing optimal electronic and mathematical properties of Buckyball nanoparticle using graph algorithms. COMPEL - The international journal for computation and mathematics in electrical and electronic engineering. 2012;31(2):387-400.
[37] Yavuz AE, Haman Bayarı S, Kazancı N. Structural and vibrational study of maprotiline. Journal of Molecular Structure. 2009;924-926:313-21.
[38] Garelli MS, Kusmartsev FV. Buckyball quantum computer: realization of a quantum gate. The European Physical

Journal B - Condensed Matter and Complex Systems. 2005;48(2):199-206.
[39] Spector PE, Fox S, Penney LM, Bruursema K, Goh A, Kessler S. The dimensionality of counterproductivity: Are all counterproductive behaviors created equal? Journal of Vocational Behavior. 2006;68(3):446-60.
[40] Ceulemans A, Muya JT, Gopakumar G, Nguyen MT. Chemical bonding in the boron buckyball. Chemical Physics Letters. 2008;461(4):226-8.
[41] Muya JT, Nguyen MT, Ceulemans A. Quantum chemistry study of symmetric methyne substitution patterns in the boron buckyball. Chemical Physics Letters. 2009;483(1):101-6.
[42] Jo S, Kim S, Lee BH, Tandon A, Kim B, Park SH, et al. Fabrication and Characterization of Finite-Size DNA 2D Ring and 3D Buckyball Structures. International Journal of Molecular Sciences. 2018;19(7).
[43] Xu J, Li Y, Xiang Y, Chen X. Energy absorption ability of buckyball C720 at low impact speed: a numerical study based on molecular dynamics. Nanoscale Research Letters. 2013;8(1):54.
[44] Rahman H, Hossain MR, Ferdous T. The recent advancement of low-dimensional nanostructured materials for drug delivery and drug sensing application: A brief review. Journal of Molecular Liquids. 2020;320:114427.
[45] Shirai Y, Osgood AJ, Zhao Y, Kelly KF, Tour JM. Directional Control in Thermally Driven Single-Molecule Nanocars. Nano Letters. 2005;5(11):2330-4.
[46] Frisch M, Trucks G, Schlegel H, Scuseria G, Robb M, Cheeseman J, et al. Gaussian 16. Gaussian, Inc. Wallingford, CT; 2016.
[47] Lee C, Wei X, Kysar Jeffrey W, Hone J. Measurement of the Elastic Properties and Intrinsic Strength of Monolayer Graphene. Science. 2008;321(5887):385-8.